International Journal of Pharmaceutics 386 (2010) 6–14

Contents lists available at ScienceDirect

International Journal of Pharmaceutics

journal homepage: www.elsevier.com/locate/ijpharm

Inhalation performance of pollen-shape carrier in dry powder formulation with different drug mixing ratios: Comparison with lactose carrier

Meer Saiful Hassan, Raymond Lau*

School of Chemical and Biomedical Engineering (SCBE), Nanyang Technological University (NTU), 62 Nanyang Drive, Singapore 637459, Singapore

ARTICLE INFO

Article history:
Received 20 July 2009
Received in revised form 7 October 2009
Accepted 25 October 2009
Available online 14 November 2009

Keywords:
Dry powder inhalation
Drug carrier
Pollen-shape
Drug mixing ratio
Emitted dose
Fine particle fraction

ABSTRACT

In this study, the drug delivery performance of pollen-shape hydroxyapatite (HA) carriers is assessed and compared with conventional lactose (LA) carriers. Budesonide (Bd) is used as the model drug. Three drug mixing ratios of 2:1, 10:1 and 45:1 (carrier:drug, w/w) are used. The attachment of the drug with the carrier is characterized by sieving test. It is found that the drug content in the blends with HA particles is higher than the blends with LA. *In vitro* inhalation experiments are also conducted in an Andersen cascade impactor (ACI) equipped with a Rotahaler® at gas flow rates of 30 and 60 L/min. The HA blends show high emitted dose (ED) of 82–90% at 30 L/min while the LA blends are observed to have ED of 69–82% at the same conditions. The high emission of the HA blends also allows high fine particle fraction (FPF) of 10–18% while the FPF of the LA blends are 3–15%. At a gas flow rate of 60 L/min, all the HA and LA blends show compatible ED (83–95% for HA blends and 82–84% for LA blends) and FPF (19–41% for HA blends and 21–34% for LA blends).

1. Introduction

For effective dry powder inhalation, drug particles need to be delivered to the alveoli region of the lung. Generally drug particles with a size of 1–5 μm are the most effective for delivery to the deep lung (Edwards, 2002). However, the attractive van der Waals force of the small particles limits their dispersion behavior. Therefore, drug particles are mixed physically with larger size carrier particles. Large carrier particles have relatively low interaction force and they can be dispersed easily. The drug particles attached to the carrier surfaces can then be carried from the inhaler to the human oral airways. As the mixture flows into the human airways, the drugs can be detached from the carriers. Drug liberation occurs due to the shear forces induced in the airways. Therefore, both high shear force (induced by high inhalation rate) (French et al., 1996) and high time of flight (long time for drug liberation) (Larhrib et al., 2006) can improve drug liberation and deep lung deposition. The carriers would eventually deposit in the upper airways while the detached drug particles can travel further to the lower airways. The physical characteritics of the carrier particles is thus a very important factor for efficient drug delivery. It is important to investigate the effect of carrier particle characteristics on the drug attachment and detachment for better control and improved drug deposition in the lower airways.

The effectiveness of carrier particles depends on the particle size, shape, surface properties and other factors (Li et al., 2004). A wide carrier particle size range of 10–220 μm (Guchardi et al., 2008; Heng et al., 2000; Iida et al., 2001; Kawashima et al., 1998; Podczeck, 1999; Srichana et al., 1998; Zeng et al., 2001) is reported in previous literature studies for dry powder inhalation. Nonetheless, the most efficient size range for carrier particles remains unclear (Bell et al., 1971; French et al., 1996; Islam et al., 2004; Steckel and Müller, 1997). It is also reported in the literature that an increase in the elongation ratio of carrier particles increases the surface area and due to the higher particle–particle interaction would reduce the drug emission. However, elongated particles have higher probability to travel further in the air stream and can help improve the overall respirable fraction of drug (Larhrib et al., 2003a,b; Zeng et al., 2000). The effect of carrier surface properties on drug inhalation efficiency is also not fully understood. A smooth carrier surface has stronger adhesion force on the drug particles and would increase the emitted dose(Kawashima et al., 1998). However, due to the limited separation of the drugs from the carrier, a reduction in particle respirable fraction is observed by some researchers (Flament et al., 2004; Heng et al., 2000; Iida et al., 2001), though the opposite is also found by others (Ganderton, 1992; Zeng et al., 2000). The drug content uniformity and stability are found to be better for particles with rough surfaces (Flament et al., 2004; Zeng et al., 2000).

Pollen-shape particles with spiky surface morphology can be a good candidate as drug carrier for dry powder inhalation. Crowder et al. (2002) suggested that drugs with surface morphologies such as pollen-like can have low van der Waals forces and may have

* Corresponding author. Tel.: +65 63168830; fax: +65 67947553.
E-mail address: wmlau@ntu.edu.sg (R. Lau).

0378-5173/$ – see front matter © 2009 Elsevier B.V. All rights reserved.
doi:10.1016/j.ijpharm.2009.10.047

excellent dispersion properties. It is also found that carrier particles with a hairy surface have longer time of flight, higher drug attachment, better drug liberation ability and exhibit better drug emission and respirable fraction (Larhrib et al., 2006). A previous study showed that the pollen-shape hydroxyapatite (HA) carriers are capable of high drug attachment (Hassan and Lau, in press). In this study, the effect of drug attachment and inhalation flow rate on the aerosolization and deposition properties of the pollen-shape HA carriers are investigated for different drug mixing ratios. HA particles are synthesized into pollen morphology with a geometric size range of 48.6 μm. The *in vitro* aerosolization and deposition properties of budesonide (Bd) blended with pollen-shape HA carriers are compared to that blended with traditional lactose (LA) carriers with three different drug mixing ratios at 30 and 60 L/min inhalation flow rate.

2. Experimental

2.1. Preparation of HA

Pollen-shape hydroxyapatite (HA, $Ca_5(PO_4)_3(OH)$) particles are synthesized by hydrothermal reaction using potassium dihydrogen phosphate (KH_2PO_4, Merck, Singapore), calcium nitrate tetrahydrate ($Ca(NO_3)_2{\cdot}4H_2O$, Sigma–Aldrich, Singapore), poly(sodium-4-styrene-sulfonate) (PSS, Aldrich, Singapore), and urea (1st Base, Singapore) (Wang et al., 2009). 30 mL of KH_2PO_4 (0.02 M) solution is added with 50 mL of $Ca(NO_3)_2{\cdot}4H_2O$ (0.02 M) solution. PSS is then added to the mixture to get a concentration of 40 g/L. Urea is added to get a concentration of 0.5 M and the mixture is stirred gently for half an hour to dissolve the urea properly. The mixture is placed in an oven at 120 °C. For the synthesis a reaction time of 6 h is used. Finally, the precipitated product is collected, washed and then dried at 70 °C.

2.2. Preparation of LA

α-Lactose monohydrate (Sigma–Aldrich, Singapore) is used as the control carrier for comparison with the performance of pollen-shape HA carriers. The LA particles are separated into a size range of 38–75 μm by sieving with a mechanical shaker (Retsch GmbH, Haan, Germany). 20 g of the LA sample is sieved using 38 and 75 μm sieves. The sieved LA is then dried in an oven at 70 °C overnight before further investigation.

2.3. Mean particle diameter and particle shape

The pollen-shape HA particle sizes are measured by laser diffraction using a Mastersizer 2000 (Malvern Instruments Ltd., Malvern, Worcestershire, UK). The samples are dispersed in 1% IPA solution in distilled water prior to the measurement. The sonicator inside the sampling chamber of the particle sizer ensures the homogeneity of the particles in the suspension. Each sample is measured in triplicate. The laser diffraction data obtained are expressed in terms of particle diameter at 10%, 50% and 90% of the volume distribution. The span of the volume distribution is estimated by the equation:

$$\text{span} = \frac{d(90\%) - d(10\%)}{d(50\%)} \quad (1)$$

The span is a representation of the homogeneity of the size distribution of the samples.

Shape, surface morphology and size of all the carrier particles are also characterized by using scanning electron microscope (SEM) (JSM-5600, JEOL, Tokyo, Japan). The dry particles are dispersed on a carbon tape attached on a stub. Then the particles are coated with platinum under an argon atmosphere (JFC-1600, JEOL, Auto Fine Coater, Tokyo, Japan) for 60 s with a current 20 mA. Then the coated particles are examined under SEM. The SEM images are taken randomly from different areas of the samples. The images are analyzed to get the distribution of the geometrical size of the particles. Dimensions of over 200 particles are measured for each sample. The surface morphologies of the particles are assessed qualitatively based on the SEM images.

2.4. Powder density

Bulk (ρ_{bulk}) and tap (ρ_{tap}) densities are important properties of dry powder samples. ρ_{bulk} and ρ_{tap} of the experimental samples are measured according to Shi et al. (2007). 100 mg of a powder sample is measured on an analytical balance. A 1 mL micro-syringe tube containing the powder is then tapped against a tabletop by hand at a rate of about four times per second for 2000–2500 taps until no reduction of the volume of the powder is noticed. The measured density at $n = 0$ is the bulk density and at $n = 2000–2500$ is the tap density.

2.5. Crystalline structure

The crystalline structure of each carrier sample is analyzed using X-ray diffraction (XRD). Samples are shaped into a thin layer in the sample holder and then inserted in the path of X-ray. XRD analysis is performed by LabX-Shimadzu XRD6000 (Shimadzu Corporation, Kyoto, Japan) diffractometer with Cu-Kα as X-ray source ($\lambda = 1.5406$ Å). A scan rate of 0.5/min, voltage of 40 kV, current of 40 mA, and step size of 0.02 are used for the measurements.

2.6. Moisture content

Thermogravimetric analysis (TGA, Diamond TG/DTA. Perkin Elmer, MA, USA) of each carrier sample is also conducted. Moisture adsorbed on the surface of the particles is measured by this analysis. Measurements are performed using 1–2 mg of sample in an alumina crucible from 25 to 125 °C at 10 °C min^{-1} heating rate under a nitrogen atmosphere.

2.7. Specific surface area

The BET surface areas of the carrier samples are measured using Autosorb® 6B (Quantachrome Instruments, Florida, USA) surface analyzer with nitrogen adsorption method. The samples are dried in Autosorb® Degassar (Quantachrome Instruments, Florida, USA) at 80 °C for 24 h under a flow of N_2 prior to the measurement.

2.8. Blending of carrier particles with Bd

Budesonide (Sigma, Singapore) is used as the model drug in this study to assess the behavior of the carriers in blending formulation. Bd and different carriers are mixed at carrier to drug weight ratio of 2:1, 10:1, and 45:1 in a REAX top mixer (Heidolph, Kelheim, Germany) for 15 min at 1000 rpm. Each blend is prepared in 100 mg quantities.

2.9. Drug content and content uniformity

The content uniformity of each blend is examined by analyzing the quantity of Bd in the blend. Three 5 mg samples are collected randomly from each blend and dissolved in a fixed amount of solvent. A mixture of 2% nitric acid (Fluka, Singapore) solution with ethanol (Merck, Singapore) in a ratio of 3:1 (v/v) is used as the solvent. Then each solution is assayed using a UV spectrophotometer (Shimadzu Corporation, Kyoto, Japan) with a wavelength of 250 nm. Each solution is analyzed three times to obtain the average Bd content. The content uniformity for the mixtures is estimated from the

variation of the results and expressed as the coefficient of variance (CV). The CV is defined as the ratio of the standard deviation of the drug content to the average drug content in the samples as a percentage.

2.10. Drug attachment

Drug attachment capacity of each carrier is evaluated using sieving method. Sieve (Retsch GmbH, Haan, Germany) with an opening of 20 μm is used with a mechanical shaker so that only the unattached drug particles are removed from the blends. 100 mg of each blend is placed on the sieve and shaked for 30 min with a mechanical shaker. The sieved blends are collected from the sieve to measure the drug contents. Some attached drug particles may be liberated from the blend during the sieving process. These liberated drug particles would also be treated as unattached particles. Each assessment is performed in triplicate.

2.11. In vitro aerosolization and deposition properties

The *in vitro* aerosolization and deposition properties of Bd blended with different carriers are determined using an eight-staged Andersen cascade impactor (ACI) (Copley Scientific Limited, Nottingham, UK) with a Rotahaler® (Glaxo, UK) device. Pre-sieved blends are used in the ACI experiments (Flament et al., 2004; French et al., 1996; Kawashima et al., 1998; Larhrib et al., 1999; Louey et al., 2004; Srichana et al., 1998; Zeng et al., 2000). Experiments are carried out with a preseparator at air flow rates of 30 and 60 L/min. In each experiment, 8 mL of the extracting solvent is poured inside the preseparator. A coating of 1% (w/v) solution of silicon oil in hexane is used on the impaction plates to prevent particle bounce and re-entrainment. 10 ± 0.3 mg of each blend is loaded into a hard gelatin capsule (Gelatin Embedding Capsules, size 4, 0.25 cm^3, Polysciences, Inc., PA, USA) before putting into the Rotahaler®. Rotahaler® is used as the inhaler to aerosolize the powder inside the ACI. An actuation time of 4 and 8 s is used for flow rates of 60 and 30 L/min, respectively, for each capsule to completely disperse all the particles. Experimental runs are conducted in triplicate. Particles remaining in the capsule, inhaler and different parts of the ACI are extracted using the same solvent used for the blend homogeneity test mentioned in the earlier section. The solutions are also assayed in a similar way.

The *in vitro* aerosolization and deposition properties of blends are commonly characterized by two parameters, namely emitted dose (ED) and fine particle fraction (FPF). ED is defined as the mass percentage of particles delivered from the inhaler (i.e., total amount excluding those in the inhaler and capsule). FPF is defined as the amount of the particles deposited in stage 2 or lower in the cascade impactor for 30 L/min and stage 0 or lower for 60 L/min (particles <5.8 μm) as a percentage of the particles collected from all the parts of the ACI including those in the inhaler and capsule.

3. Results and discussions

3.1. Particle characteristics of HA

The SEM image and physical properties of the HA particles are shown in Fig. 1 and Table 1, respectively. It can be seen that the particles have a petal-like surface morphology. Particle tip to tip distance is measured from the SEM images and the distance is taken as the particle size. It is to note that the size distributions measured from laser diffraction measurement are volume-weighted while the size distributions measured from the SEM images are number-weighted. Therefore, the SEM size distributions are converted to volume-weighted distribution before comparisons are made. The conversion of number-weighted size distribution to volume-weighted size distribution requires the knowledge of particle volume. The volume of pollen-shape particle is assumed to be the same as a sphere having the same diameter. Hence, it can be seen from Table 1 that the SEM measured sizes are slightly higher than $d(50\%)$ of the laser diffraction measured size. The span of the HA particles is close to 1, which indicates a uniform size distribution (Li et al., 2004). The particle aerodynamic diameter, d_a shown in Table 1 is calculated using the equation:

$$d_a = d_e \sqrt{\frac{\rho_e}{\lambda \rho_s}} \quad (2)$$

where $\rho_s = 1$ g/cm^3, d_e is the particle geometric diameter, ρ_e is the effective particle density in the same unit as ρ_s and λ is the particle dynamic shape factor. The SEM measured size is used as the equivalent diameter of the particles. The tap density is used conventionally as the particle effective density (Edwards et al., 1997). The dynamic shape factor depends on the ratio of the drag force on the concerned particle and the drag force for a sphere having the same volume. The dynamic shape factor for a sphere would be 1. Since the pollen-shape would cause a higher drag than a sphere but still closely resemble a spherical shape, a dynamic shape factor of 1.1 is estimated for the pollen-shape particles. Even though the dynamic shape factor is an estimated value, the error from the estimation should have minimal effect on the calculation of the aerodynamic diameter since the aerodynamic diameter is proportional to the square root of the dynamic shape factor.

The XRD result of the HA particles is shown in Fig. 2(a). The diffraction pattern indicates the hexagonal phase of HA crystalline structure and they are consistent with the powder diffraction file (PDF) no. 00-009-0432. Diffraction peaks for foreign compounds

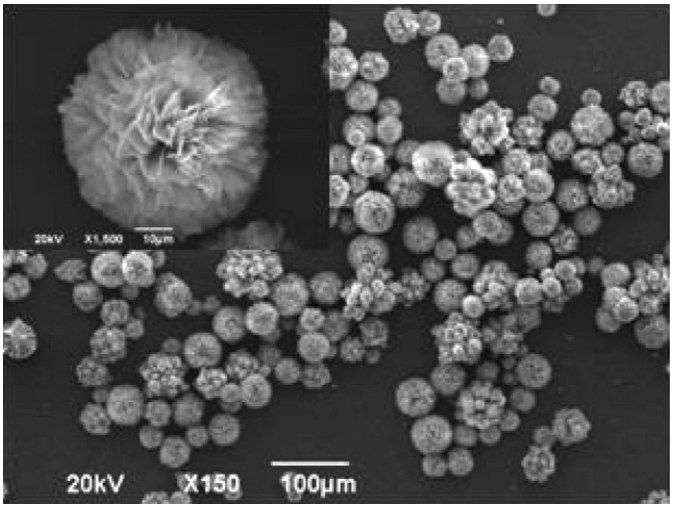

Fig. 1. The SEM image of HA.

Table 1
Physical characteristics of the HA samples.

Sample	HA
Average dia. (SEM) (μm)	48.6
St. dev. (μm)	10.21
$d(50\%)$ (μm)	45.9
$d(10\%)$ (μm)	25.9
$d(90\%)$ (μm)	85.9
Span	1.31
ρ_{bulk} (g/cm^3) ($n = 0$)	0.215
ρ_{tap} (g/cm^3) ($n = 2500$)	0.289
d_a (μm)	24.9
Specific surface area (m^2/g)	17.1

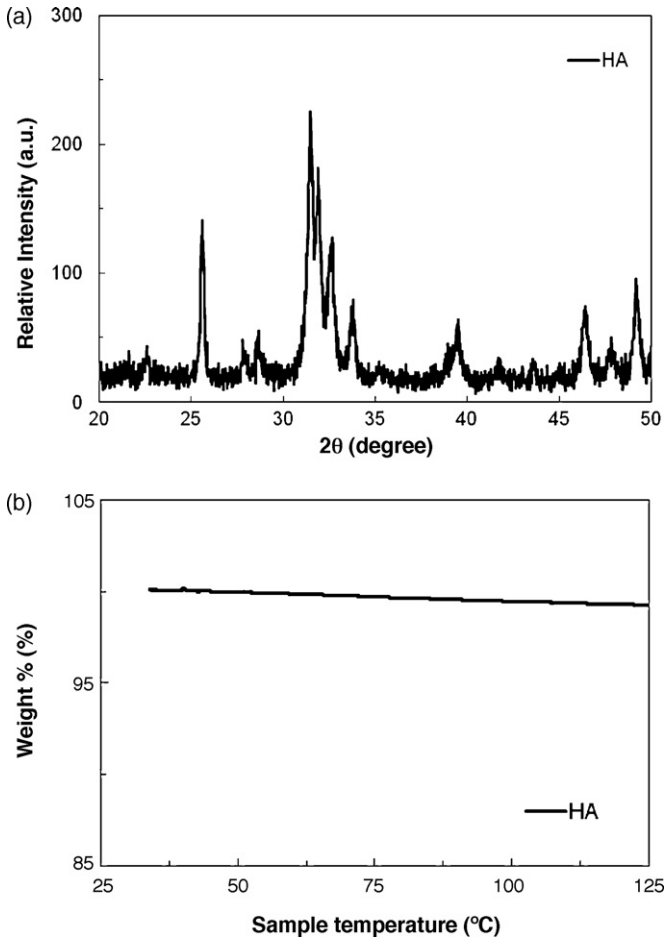

Fig. 2. (a) XRD pattern and (b) TGA spectrum of the HA sample.

are not found in the pattern. A high purity of HA is obtained by the hydrothermal method used in this study.

Moisture content in the powder samples can enhance particle aggregation tendency (Visser, 1989) and affect particle dispersion and flowability. The moisture content of the HA particles is analyzed by TGA. The TGA thermogram of the sample is shown in Fig. 2(b). The moisture content is referring to the moisture adsorbed on the surface of the particles that could influence particle–particle interaction. It can be seen that, the HA sample shows negligible weight loss (<2%) below 100 °C. It suggests that the sample contain negligible amount of free water. Therefore, the hygroscopic effect on the inhalation behavior of the sample can be considered as negligible (Larhrib et al., 1999).

3.2. Particle characteristics of LA

LA particles are sieved into a size range of 38–75 μm. It can be seen from the SEM image of the sieved LA sample in Fig. 3 that there is negligible amount of fine particles present. The physical properties of the sample are listed in Table 2. The LA particles have higher tap density than the HA particles, which would also translate to a higher aerodynamic diameter than the HA particles.

Table 2
Physical properties of the LA particles.

Sample	LA
Size range (μm)	38–75
ρ_{bulk} (g/cm^3) (n = 0)	0.586
ρ_{tap} (g/cm^3) (n = 2500)	0.874
Specific surface area (m^2/g)	9.45

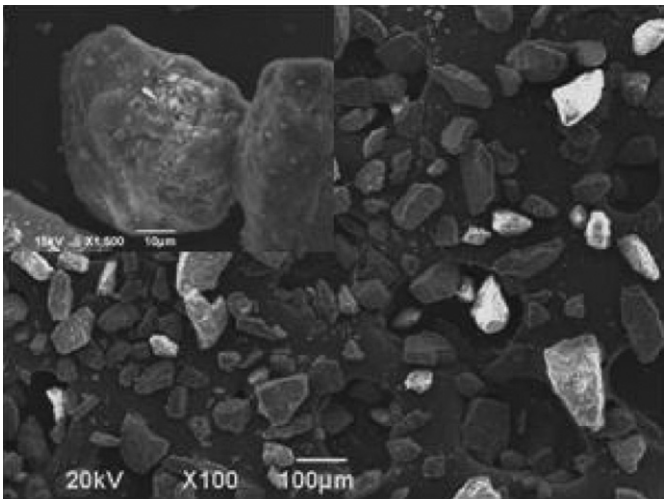

Fig. 3. SEM image of LA monohydrate with a size range of 38–75 μm.

XRD and TGA analyses are also performed for the LA sample and the result is shown in Fig. 4. The XRD pattern shows a high purity and crystallinity of the LA sample (consistent with PDF no. 00-030-1716 monoclinic). TGA spectrum also shows that the weight loss of the sample due to moisture content is negligible within 100 °C.

3.3. Drug blending

Bd is used as the model drug in this study. The SEM image of the Bd particles is shown in Fig. 5. These particles have an average

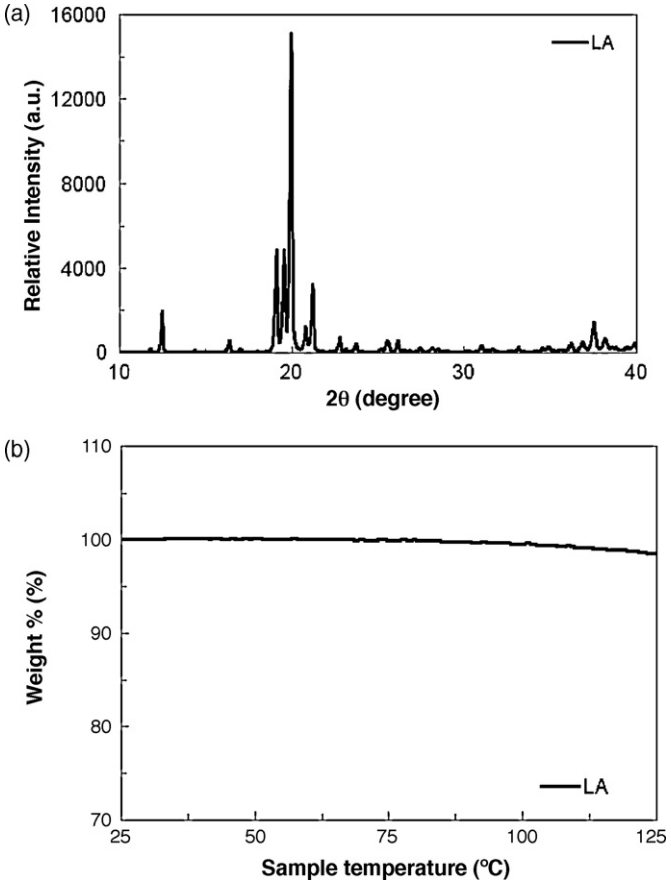

Fig. 4. (a) XRD pattern and (b) TGA spectrum of LA.

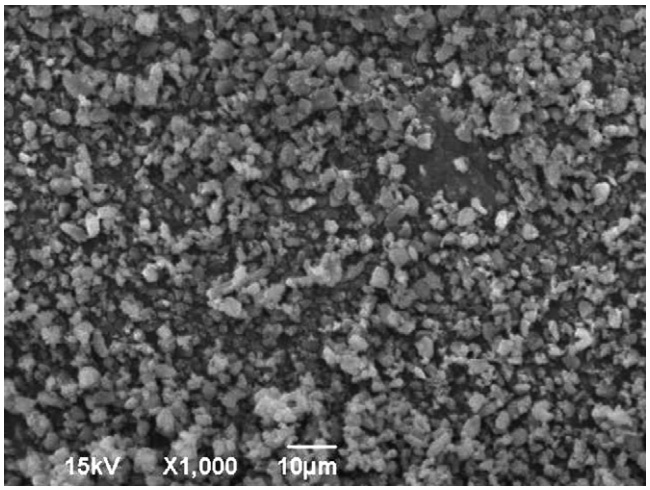

Fig. 5. SEM image of Bd.

size of 2.5 ± 1.1 μm. Bd is blended with carriers at a drug mixing ratio of 2:1, 10:1 and 45:1 (carrier:drug, w/w) in small transparent vials. The appearance of the blended Bd is compared with that of pure carrier particles. The vials with the carrier only and carrier with drug formulations are shown in Fig. 6. It can be seen from Fig. 6(a) that a substantial amount of particles are attached to the wall of the vials for all the blends with LA carriers. Since there is no obvious attachment of particles to the vial surface, it is reasonable to consider all the attached particles to be the Bd. As shown in Fig. 6(b), obvious Bd attachment on the vial surface is only observed at high drug mixing ratio of 2:1 for HA carriers.

The blends are also characterized by SEM. The SEM images for the blends with different drug mixing ratios are shown in Fig. 7. A comparison of the SEM images of the carriers (Figs. 1 and 3) and Bd (Fig. 5) indicates that the small particles in Fig. 7 would be Bd and the large particles would be the carriers. The SEM images show

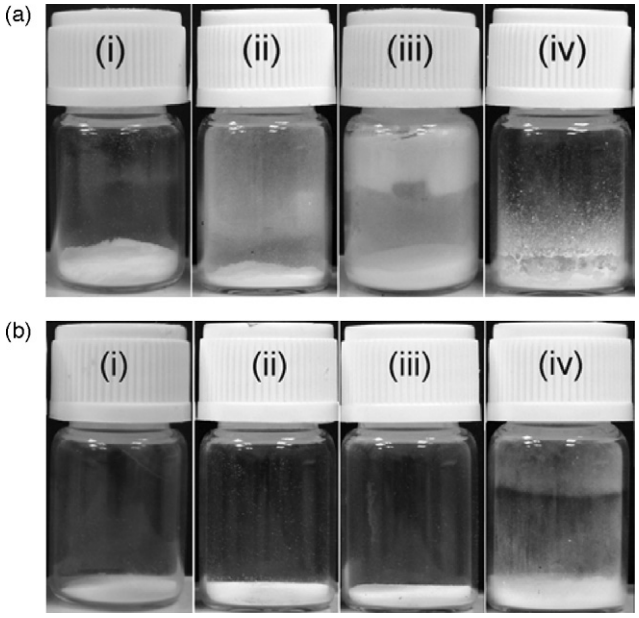

Fig. 6. Comparison of the blends in the mixture vials, with different carrier to drug mixing ratio. (a) LA carrier (i) without drug; with wt ratio (ii) 45:1, (iii) 10:1, (iv) 2:1 and (b) HA carrier (i) without drug; with wt ratio (ii) 45:1, (iii) 10:1, (iv) 2:1.

consistent results compared with the observation of drug attachment on vial surfaces. As shown in Fig. 7(a), a substantial amount of unattached Bd can be seen in the blend with LA carriers for all drug mixing ratios. For HA carriers, significant amount of unattached Bd can only be seen at high drug mixing ratio of 2:1 indicated in Fig. 7(b). It is believed that the pollen morphology of HA carriers is the main contributor of the better drug attachment than LA carriers. The petal-like surfaces of HA allow the attachment of larger amount of Bd compared to the relatively flat LA surfaces.

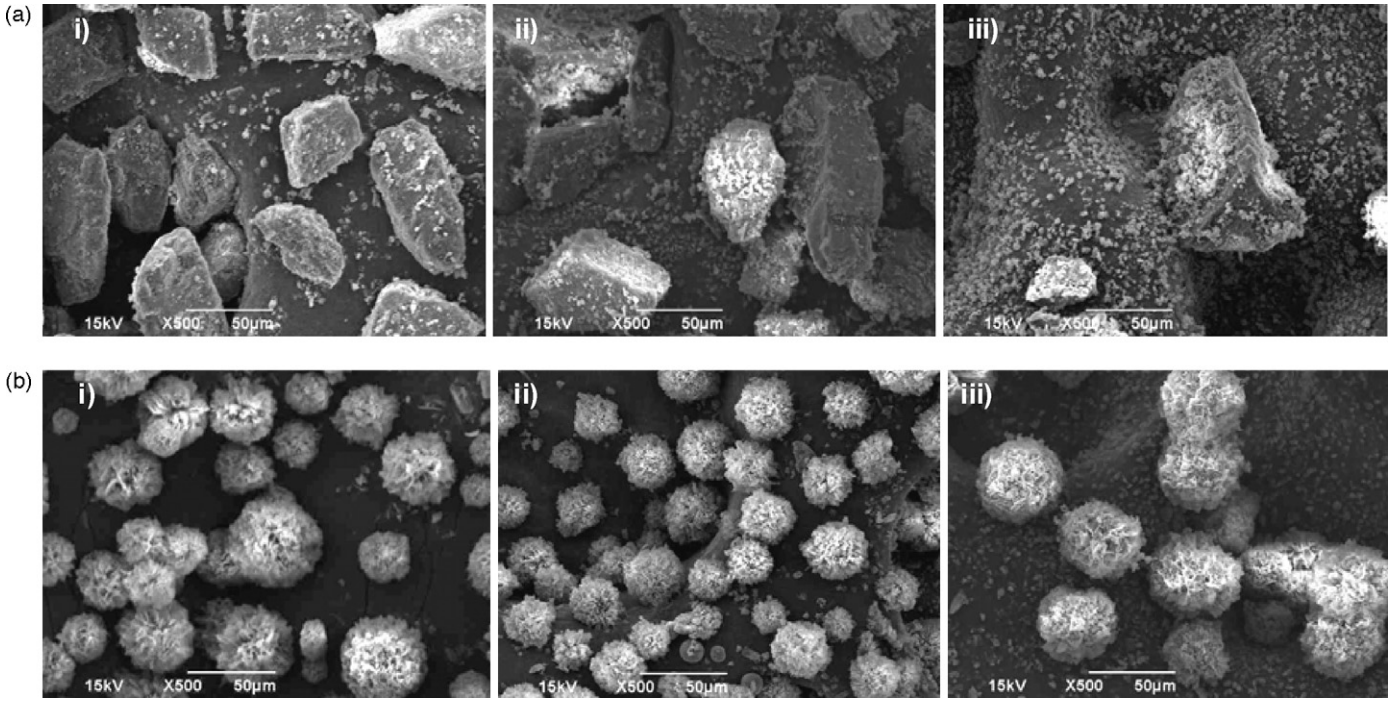

Fig. 7. Comparison of the blends of the three carriers with Bd with different drug mixing ratios. (a) LA carrier with ratio (i) 45:1, (ii) 10:1, (iii) 2:1 and (b) HA carrier with ratio (i) 45:1, (ii) 10:1, (iii) 2:1.

Table 3
Average Bd content and homogeneity of the blends.

Wt ratio (carrier:drug)	Carrier	Wt fraction of drug (wt%)	CV (%)
2:1	LA	23.0	7.87
	HA	22.5	0.26
10:1	LA	7.9	2.99
	HA	8.9	2.14
45:1	LA	1.73	0.95
	HA	1.81	6.26

3.4. Blending homogeneity

The homogeneity of the blends can be represented by the CV of the Bd content in the blends. The average drug content and CV for the blends after mixing are listed in Table 3. It is found that the blend homogeneity increases with an increase in drug mixing ratio for HA carriers while the opposite is observed for LA carriers. The opposite effect of drug mixing ratio on the blend homogeneity of the carriers is anticipated to be due to the number of sites available for drug attachment. For LA carriers, there is limited number of sites and they will be occupied by the drug particles easily at low drug mixing ratios. An increase in drug mixing ratio would thus reduce the blend homogeneity. On the other hand, HA carriers have large number of sites. During the blending step, drug particles will be attached to the first available site and at low drug mixing ratio, the attachment may not be uniform. As the drug mixing ratio is increased, the sites would be occupied more uniformly and the blend homogeneity is increased. Though the blend homogeneity of the samples exhibits some variations, all the CV values are lower than 8%. Therefore, the blends are considered as homogenous (Flament et al., 2004; Larhrib et al., 2003a; Louey et al., 2004).

3.5. Drug attachment

From the SEM images of Fig. 7, it can be seen that a certain amount of drugs are not attached onto the carrier surfaces. The unattached drugs may attach to the inhaler surfaces and cause unnecessary loss of expensive drugs. Therefore, the drug attachment characteristic on carriers is very important for effective usage of the formulation. Sieving tests are performed for the different blends and the drug contents before and after sieving are compared. The average drug content in the samples and the % CV of the samples after sieving are listed in Table 4. It can be seen that the average drug content is significantly lower for LA particles than the HA particles after sieving except a high drug mixing ratio of 2:1. For drug mixing ratio of 45:1 and 10:1, the LA blends show a substantial reduction in average drug content after sieving. On the other hand, HA particles show a fairly low reduction. At a high drug mixing ratio of 2:1, the surfaces of the carrier particles are fully covered with drug particles. The excess unattached drug particles may form aggregates and limit the physical separation. Therefore, reductions in the drug content from these two blends with ratio 2:1 are not significantly different. It is also noticed that the homogeneity of the blends reduces after sieving. A minor variation in drug content may be observed because the drug content after sieving depends on different factors like the storage time and condition, sieving time and condition, the degree of mixing, etc. It is believed that drug attachment ability of the carrier particles is proportional to carrier surface area. The BET surface areas of the carriers are shown in Tables 1 and 2. The average opening diameter among the petals is found to be around 5 μm while the average drug particles size is around 3 μm. It would be reasonable to assume that the drug particles would have access to most of the surface area of the petal like morphology of the HA carriers.

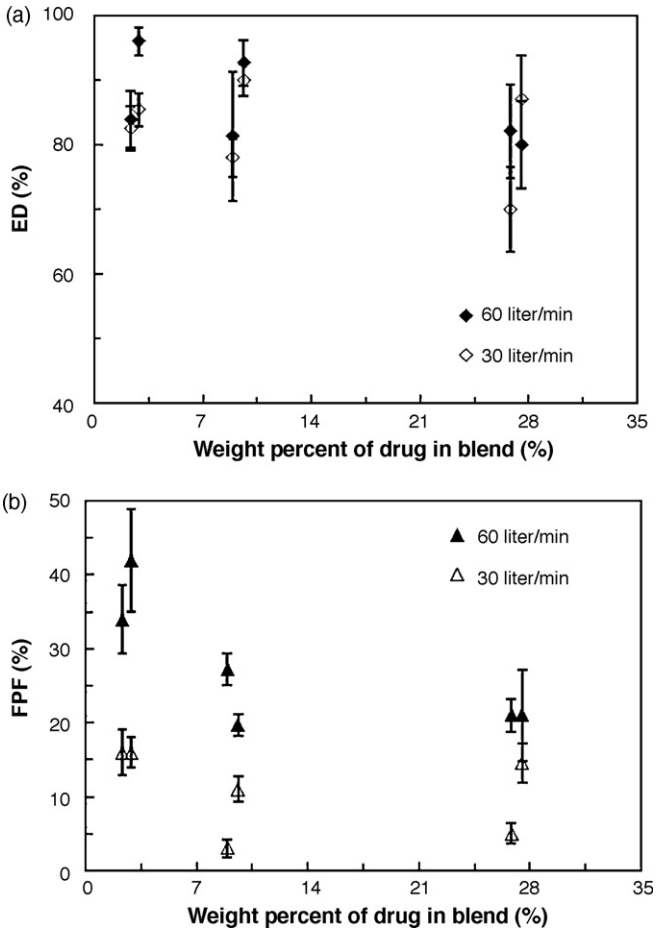

Fig. 8. (a) Emitted dose and (b) fine particle fraction of the blends with different drug weight percentages obtained from homogeneity test for 60 and 30 L/min.

3.6. In vitro deposition behavior of blending formulations with different drug mixing ratios

The ED and FPF results obtained from the ACI experiments are plotted as a function of the weight percent of drug in the blend and shown in Fig. 8. The weight percent of drug in the blend is

Table 4
Attachment of Bd drug with LA and HA carriers.

Wt ratio (carrier:drug)	Carrier	After sieving		Reduction in drug content (wt%)
		Wt fraction of drug (wt%)	CV (%)	
2:1	LA	12.9	13.5	43.8
	HA	13.9	3.84	38.3
10:1	LA	4.35	3.76	52.5
	HA	7.55	4.84	27.0
45:1	LA	0.62	7.73	62.2
	HA	1.72	11.8	20.7

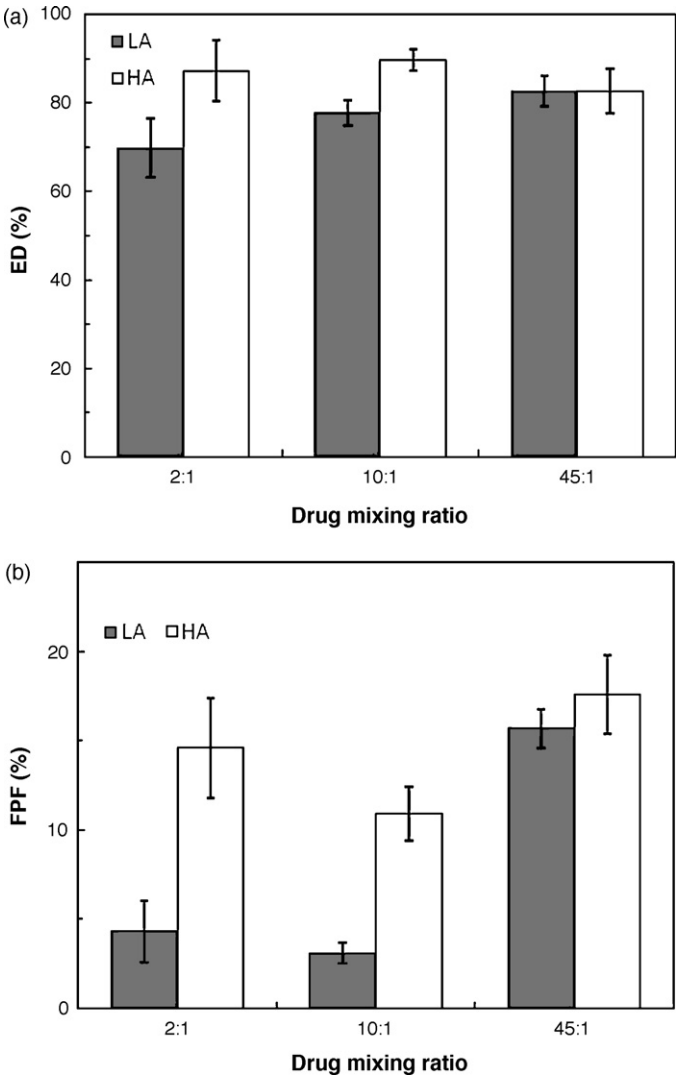

Fig. 9. (a) Emitted dose and (b) fine particle fraction of blends with carrier to drug mixing ratio 2:1, 10:1 and 45:1 at 30 L/min.

obtained from the blend homogeneity test (Table 3). In Fig. 8(a), the ED results do not seem to be a strong function of weight percent of drug. However, blends with a higher drug percentage show a slightly lower average ED. A flow rate of 60 L/min is found to provide slightly higher ED than a flow rate of 30 L/min. A higher flow rate generates higher shear force, which improves the aerosolization of the drug particles (French et al., 1996). It can be seen in Fig. 8(b) that FPF decreases with an increase in drug mixing ratio. Gas flow rate has a more significant effect on the FPF than the ED. FPF at 60 L/min is substantially higher than that at 30 L/min. The increased shear force at higher gas flow rate does not only improve the aerosolization of the blend but also improves the liberation of the drug particles as well, thus allow more drug particles to travel to the lower stages.

A certain variation in ED and FPF can be observed at similar drug weight percentage since different carriers are used. It would be beneficial to analyze the emission and deposition properties of the each carrier separately. The ED and FPF results at a flow rate of 30 L/min for the different blends are compared separately in Fig. 9. The LA blends are found to give lower ED than the HA blends at a flow rate of 30 L/min especially at high drug mixing ratios of 2:1 and 10:1. It is believed to be due to the high amount of unattached drug particles in the LA blends. LA particles can attach lower number of

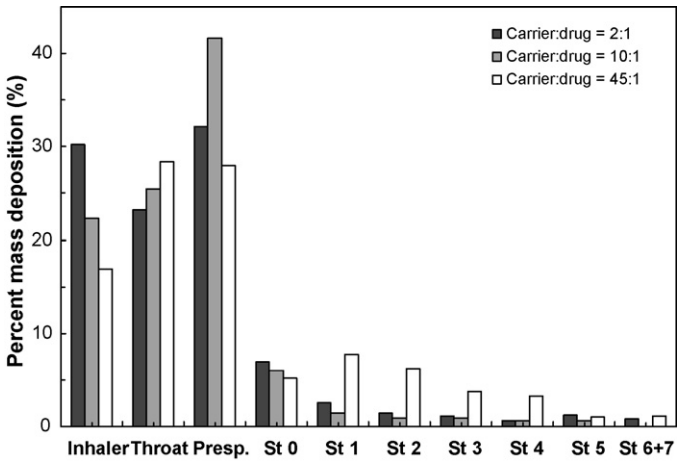

Fig. 10. Detailed deposition of the drug from the LA blends with different carrier to drug mixing ratio at 30 L/min.

drug particles due to their lower surface area. On the other hand, the morphology of HA carriers allows the attachment of more drug particles than the LA carriers. Lower amount of unattached drug would be lost in the inhaler and therefore a higher ED is observed.

Similar to the ED result, the FPF of the LA blend is also lower than that of the HA blends as shown in Fig. 9(b). The low FPF of the LA blends is a result of low emission from the inhaler. While the aerodynamic diameter of both LA and HA particles is high enough not to penetrate into the lower stages, the FPF would only be contributed from the liberated drug particles.

The flow and deposition behavior of these blends can be comprehended based on the regional deposition results of the blends at 30 L/min. The detailed deposition results of the carrier blends with different drug mixing ratios are shown in Figs. 10 and 11. From the detailed deposition, it can be seen that the depositions are mostly happen in the initial three regions. The deposition in the inhaler is due to the attachment of drug particles on the inhaler surface. The bending at the throat region causes some of the blend to deposit due to inertial impaction. The preseparator is designed in such a way that most particles having an aerodynamic diameter larger than 10 μm will be retained. High drug deposition would be observed if carriers are deposited without sufficient drug liberation.

The regional deposition result in Fig. 10 indicates that for the LA blends a substantial amount of drug particles is deposited in the

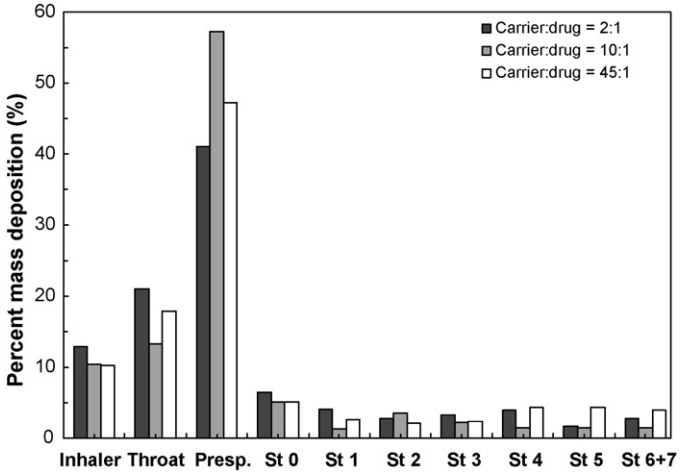

Fig. 11. Detailed deposition of the drug from HA blends with different carrier to drug mixing ratio at 30 L/min.

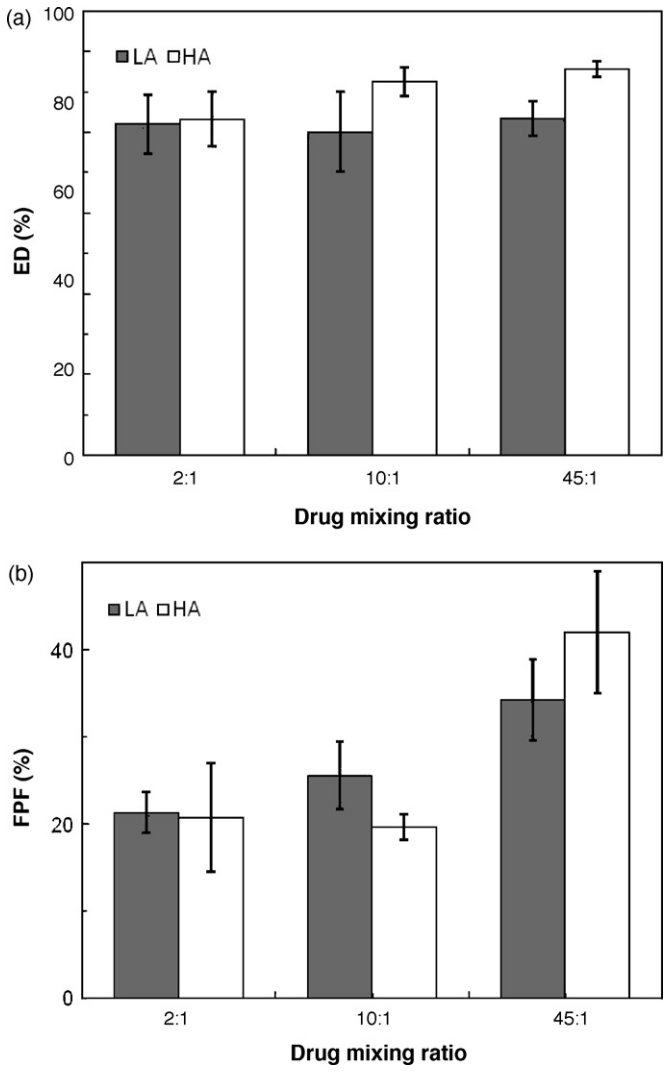

Fig. 12. (a) Emitted dose and (b) fine particle fraction of blends with carrier to drug mixing ratio 2:1, 10:1 and 45:1 at 60 L/min.

inhaler. It is reasonable considering the large amount of unattached drug particles observed in the LA blends. Additional drug deposition in the throat and preseparator would be due to the deposition of LA carriers together with drug particles not being liberated. After these three initial stages, only a small amount of drug particles are left to travel to the lower stages of the impactor and exhibit low FPFs. An increase in drug mixing ratio indicates a higher deposition at the inhaler region, which is in agreement with the observations of higher amount of unattached drug particles at higher drug mixing ratios. While more drug particles are deposited in the inhaler region at higher drug mixing ratios, less drug particles would be able to go into the system and subsequently travel to the lower stages. Thus, the ED and FPF also decrease with an increase in drug mixing ratio.

The detailed deposition results of HA blends are shown in Fig. 11. As expected, the deposition in the inhaler region for HA blends is lower than that for the LA blends due to the better drug attachment. The comparable amount of deposition in the inhaler region at drug mixing ratios of 10:1 and 45:1 for HA blends indicates that the drug attachment limit of the HA carriers has not been reached even at a relatively high drug mixing ratio of 10:1.

A flow rate of 60 L/min is also used to approximate the maximum inhalation rate of a normal adult in the dry powder inhalation process. The ED and FPF results for the blends with different carriers at a flow rate of 60 L/min are shown in Fig. 12. A flow rate of 60 L/min

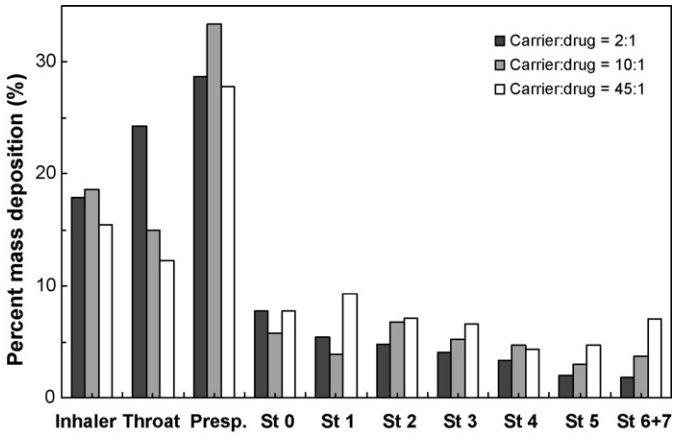

Fig. 13. Detailed deposition of the drug from LA blends with different carrier to drug mixing ratio at 60 L/min.

is found to have higher ED than 30 L/min for all formulations. An increase in the air flow rate increases the turbulence and shear forces, which in turn improves the aerosolization of the drug particles. It can be seen in Fig. 12(a) that HA blends again show higher ED than the LA blends. However, the relationship between ED and drug mixing ratios at a flow rate of 60 L/min is not as obvious as that at a flow rate of 30 L/min owing to the higher shear forces at higher flow rate. Fig. 12(b) shows that the FPF of the blends increases with the decrease of drug mixing ratio. When Fig. 12(b) is compared with Fig. 9(b), it can be seen that the LA blend has the higher increase in FPF as the gas flow rate is increased, especially at high drug mixing ratios. This is because the large shear force generated at high gas flow rate would be able to aerosolize some of the unattached drug particles. Once these unattached drug particles are aerosolized, they would be able to travel directly to the lower stages without the need of liberation. The HA blends also shows an improvement in FPF with an increase in gas flow rate. However, the improvement is not as significant as the LA blends because the HA blends does not have as much unattached drug particles. The improvement in FPF would be mainly due to the improved drug liberation at the higher gas flow rate. It is also found that the drug liberation is more effective at low drug mixing ratios that at high drug mixing ratios.

The regional deposition of the blends at 60 L/min is also shown in Figs. 13 and 14. A comparison with Figs. 10 and 11 shows that an increase in gas flow rate from 30 to 60 L/min essentially reduces the amount of drug particles deposited in the

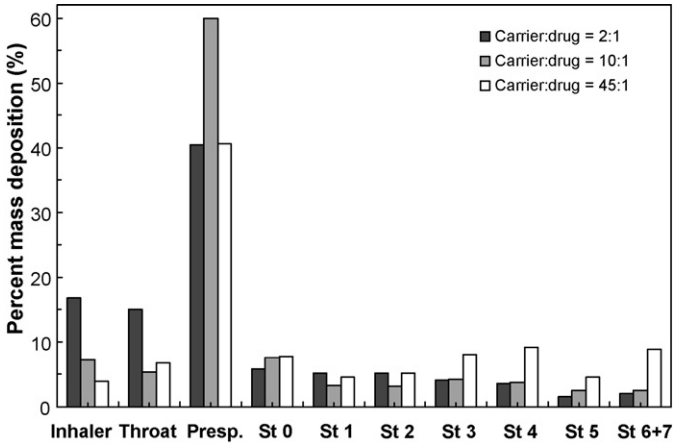

Fig. 14. Detailed deposition of the drug from HA blends with different carrier to drug mixing ratio at 60 L/min.

earlier regions. As mentioned earlier, the high gas flow rate helps improve the drug liberation from the carriers and reduces early depositions.

A summary of all the results reported in this study suggests that pollen-shape particles can be a viable choice as drug carriers in inhalation drug delivery. The pollen-shape morphology allows high drug mixing ratio without sacrificing the delivery efficiency compared to traditional LA carriers especially at lower inhalation flow rate. A much wider application of the pollen-shape carriers can be possible if the drug liberation can be improved.

4. Conclusion

The inhalation performance of pollen-shape HA carriers with a geometric diameter of 48.6 μm is compared with LA carriers with a size range 38–75 μm with different drug mixing ratios. The drug attachment ability of the HA carriers is higher than that of the LA carriers. A significant amount of the drug particles is found to remain unattached to the LA carriers. These unattached drug particles maybe lost in the inhaler and reduce the aerosolization and deposition performance of the blends. The HA blends showed significantly better ED and FPF than the LA blends at high drug mixing ratios and a gas flow rate of 30 L/min. At 60 L/min, the HA blends exhibit better ED. However, due to the low liberation of the drug particles, similar FPF with the LA blends is observed. This study shows the suitability of pollen-shape carriers especially at a low flow rates and high drug mixing ratios. The liberation of drug particles from the pollen-shape carriers needs to be improved for a more diverse application of pollen-shape carriers.

Acknowledgement

The authors are grateful to the financial support of NTU/SUG Grant.

References

Bell, J.H., Hartley, P.S., Cox, J.S.G., 1971. Dry powder aerosols. I. A new powder inhalation device. J. Pharm. Sci. 60, 1559–1564.
Crowder, T.M., Rosati, J.A., Schroeter, J.D., Hickey, A.J., Martonen, T.B., 2002. Fundamental effects of particle morphology on lung delivery: predictions of stokes' law and the particular relevance to dry powder inhaler formulation and development. Pharm. Res. 19, 239–245.
Edwards, D.A., 2002. Delivery of biological agents by aerosols. AIChE J. 48, 2–6.
Edwards, D.A., et al., 1997. Large porous particles for pulmonary drug delivery. Science 276, 1868.
Flament, M.-P., Leterme, P., Gayot, A., 2004. The influence of carrier roughness on adhesion, content uniformity and the in vitro deposition of terbutaline sulphate from dry powder inhalers. Int. J. Pharm. 275, 201–209.
French, D.L., Edwards, D.A., Niven, R.W., 1996. The influence of formulation on emission, deaggregation and deposition of dry powders for inhalation. J. Aerosol Sci. 27, 769–783.
Ganderton, D., 1992. The generation of respirable cloud from coarse powder aggregates. J. Biopharm. Sci. 3, 101–105.
Guchardi, R., Frei, M., John, E., Kaerger, J.S., 2008. Influence of fine lactose and magnesium stearate on low dose dry powder inhaler formulations. Int. J. Pharm. 348, 10–17.
Hassan, M.S., Lau, R., in press. Feasibility study of pollen-shape drug carriers in dry powder inhalation. J. Pharm. Sci., doi:10.1002/jps.21913.
Heng, P.W.S., Chan, L.W., Lim, L.T., 2000. Quantification of the surface morphologies of lactose carriers and their effect on the in vitro deposition of salbutamol sulphate. Chem. Pharm. Bull. 48, 393–398.
Iida, K., Hayakawa, Y., Okamoto, H., Danjo, K., Leuenberger, H., 2001. Evaluation of flow properties of dry powder inhalation of salbutamol sulfate with lactose carrier. Chem. Pharm. Bull. 49, 1326.
Islam, N., Stewart, P., Larson, I., Hartley, P., 2004. Effect of carrier size on the dispersion of salmeterol xinafoate from interactive mixtures. J. Pharm. Sci. 93, 1030–1038.
Kawashima, Y., Serigano, T., Hino, T., Yamamoto, H., Takeuchi, H., 1998. Effect of surface morphology of carrier lactose on dry powder inhalation property of pranlukast hydrate. Int. J. Pharm. 172, 179–188.
Larhrib, H., Cespi, M., Dyas, M.A., Roberts, M., Ford, J.L., 2006. Engineered carrier with a long time of flight (TOF) to improve drug delivery from dry powder inhalation aerosols. Drug delivery to the Lungs (DDL) 17, 304–307.
Larhrib, H., Martin, G.P., Marriott, C., Prime, D., 2003a. The influence of carrier and drug morphology on drug delivery from dry powder formulations. Int. J. Pharm. 257, 283–296.
Larhrib, H., Martin, G.P., Prime, D., Marriott, C., 2003b. Characterisation and deposition studies of engineered lactose crystals with potential for use as a carrier for aerosolised salbutamol sulfate from dry powder inhalers. Eur. J. Pharm. Sci. 19, 211–221.
Larhrib, H., Zeng, X.M., Martin, G.P., Marriott, C., Pritchard, J., 1999. The use of different grades of lactose as a carrier for aerosolised salbutamol sulphate. Int. J. Pharm. 191, 1–14.
Li, Q., Rudolph, V., Weigl, B., Earl, A., 2004. Interparticle van der Waals force in powder flowability and compactibility. Int. J. Pharm. 280, 77–93.
Louey, M., Van Oort, M., Hickey, A., 2004. Aerosol dispersion of respirable particles in narrow size distributions using drug-alone and lactose-blend formulations. Pharm. Res. 21, 1207–1213.
Podczeck, F., 1999. The influence of particle size distribution and surface roughness of carrier particles on the in vitro properties of dry powder inhalations. Aerosol Sci. Technol. 31, 301–321.
Shi, L., Plumley, C.J., Berkland, C., 2007. Biodegradable nanoparticle flocculates for dry powder aerosol formulation. Langmuir 23, 10897–10901.
Srichana, T., Martin, G.P., Marriott, C., 1998. On the relationship between drug and carrier deposition from dry powder inhalers in vitro. Int. J. Pharm. 167, 13–23.
Steckel, H., Müller, B.W., 1997. In vitro evaluation of dry powder inhalers II: influence of carrier particle size and concentration on in vitro deposition. Int. J. Pharm. 154, 31–37.
Visser, J., 1989. Van der Waals and other cohesive forces affecting powder fluidization. Powder Technol. 58, 1–10.
Wang, Y., et al., 2009. Polyelectrolyte mediated formation of hydroxyapatite microspheres of controlled size and hierarchical structure. J. Colloid Interf. Sci. 339, 69–77.
Zeng, X.-M., Martin, G.P., Marriott, C., Pritchard, J., 2001. Lactose as a carrier in dry powder formulations: the influence of surface characteristics on drug delivery. J. Pharm. Sci. 90, 1424–1434.
Zeng, X.M., Martin, G.P., Marriott, C., Pritchard, J., 2000. The influence of carrier morphology on drug delivery by dry powder inhalers. Int. J. Pharm. 200, 93–106.